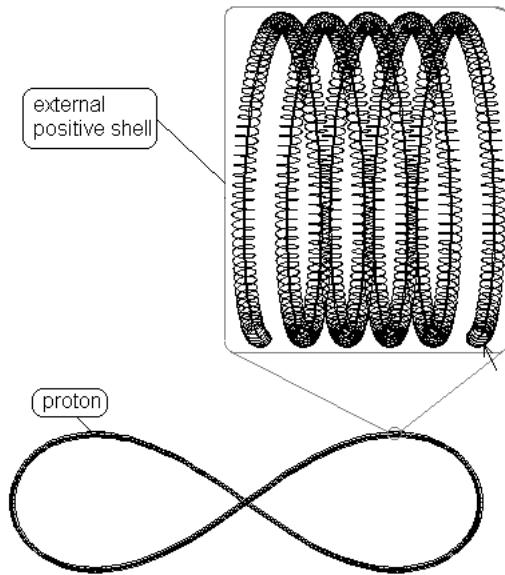


Chapter 7. Hydrogen atom

The Hydrogen atom is a dynamical system composed of one proton and one electron. The internal structures and individual properties of both particles were discussed extensively in the previous Chapters 3 and 6. The analysis of the dynamical properties of the Hydrogen atom, is very useful for understanding the structure and dynamical properties of other atoms.

7.1 Proton as a nucleus of the Hydrogen atom

The proton is a $TTH_1^3: +(-)$, a twisted closed loop helical structure (with external shape like the digit 8) enclosing a pair of internal pions and one kaon. Its internal structure was shown in Fig. 2.15.B. The proton shape (illustrated in Fig. 6.22 of Chapter 6) is shown again in the figure below.



[Fig. 6.22]
Proton shape

The proton core is a three dimensional curve, whose plane projection is given by the Hippoped curve at parameter $a = \sqrt{3}$. The analytical expressions of the Hippoped curve (in polar and Decart system) were given in Chapter 6 (Eq. 6.54.a and 6.54.b). The plot of this curve with some specific dimensions, is shown in Fig. 7.1. We may call the two portions of the curve **proton clubs**. While the real proton clubs do not lie in a plane but in a slightly curved surface, we may call this surface a quasi-

plane. It is slightly curved, because the core length to thickness ratio of the proton (also the neutron) is:

$$L_{pc}/2(R_c + r_p) = 207.6$$

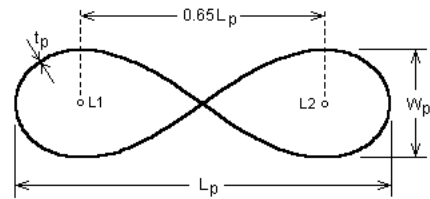


Fig. 7.1

Projection of the proton core on a 2D plane

The dimensions of the proton core, determined in §6.12.2.6 are following:

$$L_p = 0.667 \times 10^{-10} \text{ (m) - proton length} \quad (6.76)$$

$$W_p = 0.19253 \times 10^{-10} \text{ (m) - proton width} \quad (6.77)$$

$$t_p = 2(R_c + r_p) = 7.8411 \times 10^{-13} \text{ (m) - core thickness} \quad (6.78)$$

$$L_{pc} = 1.62772 \times 10^{-10} \text{ (m) - core length}$$

The ratio between the length and width of the curve for the accepted parameter $a = \sqrt{3}$ is 3.4643. There are two characteristic points in the proton quasiplane, shown in Fig. 7.1 as L_1 and L_2 . They are located on the horizontal axis passing through the geometrical centre and corresponds to a maximal vertical width. The distance between them is $0.648L_p$. These points, called **locuses**, are characteristic points for the distributed proximity electrical field of the proton.

7.2 Bohr surface of the Hydrogen atom

7.2.1 Proton electrical field

The proton core structure was described in details in Chapter 6. The positive charge is contributed by the RL(T) of the external shell. Having in mind the finite dimensions and shape of the proton core, the electrical charge in the closed field is distributed over the external shell. The unit electrical charge is a result of the IG energy balance between the RL(T) structures of the proton's helical structures and the surrounding CL space. In the far field the electrical lines appear radial to the geometrical

centre of the Hippoped curve and their density distribution simulates a point charge. In the near field, however, the electrical lines are curved with a spatial configuration determined by the proton core shape. Consequently, when approaching the proton from the far field, some boundary range should exist, beyond which the straight radial electrical lines are converted to curve lines. We may approximate this boundary range with an equivalent surface. Outside of this surface, the proton will look like a point charge particle, possessing the Newtonian mass of the proton. So it should be a closed surface. Inside of this surface the proton's electrical field will not converge to a point charge but to the proton core (Note: the proton core should not be confused with its internal core. The proton core is the external enclosure of the twisted helical structure of the proton, which thickness is $2(R_c + r_p)$).

7.2.2 Relation between the BSM model of the Hydrogen atom and Bohr model

The Quantum mechanics is successfully built on the concept of the Bohr model of the Hydrogen atom. According to BSM theory, the Quantum Mechanical (QM) models of the Hydrogen and other atoms are good **mathematical models**, providing very useful quantum features. However, they could not serve as physical models of the atomic structure. The main discrepancy comes from the absence of CL space parameters and the structural features of the elementary particles in the QM models. The goal of the BSM theory is to provide exact physical model of the Hydrogen and other atoms. One useful parameter, that the BSM model will use from the Bohr model is the Bohr radius, denoted as a_o . The proper use of this parameter will provide an useful bridge between the quantum model of the atoms and the BSM physical models.

In §3.12.2 the parameter a_o was determined from the conditions defining the quantum orbit length (Eq. (3.43.f) and (3.43.g). In the same time a_o is determined by the Bohr model of the Hydrogen atom.

$$a_o = \frac{h^2 \epsilon_o}{\pi m_e q^2} \quad (7.1)$$

Then we have:

$$\frac{h^2 \epsilon_o}{\pi m_e q^2} = a_o = \frac{\lambda_c}{2\pi\alpha} \quad (7.2)$$

The left side relation is from the Bohr model of Hydrogen, while the right side is related to the quantum orbit equivalent radius for electron quantum motion with first harmonic velocity. Based on the a_o parameter, the Eq. (7.1) provides very useful relation between the CL space parameters, the Plank constant and the unit charge. Multiplying the nominators of relations (7.2) by 2π , we obtain relation valid for the first harmonic quantum orbit, whose length is equal to $2\pi a_o$.

$$\frac{2h^2 \epsilon_o}{m_e q^2} = \frac{\lambda_c}{\alpha} = 2\pi a_o = const \quad (7.3)$$

The ground state orbit in Bohr model defines a spherical surface around the point like proton with radius a_o . The proton shape according to BSM is quite different, and the ground state orbit will define a surface different than sphere. The equivalence of Eq. (7.2) and (7.3) allows us to use the spherical surface area, defined by the radius a_o , as a modified characteristic parameter of the quantum orbit condition. In such case the radius a_o provides a bridge between the Bohr and the BSM model of the Hydrogen atom. In order to preserve (at least approximately) the relation to the Bohr model, we will make the area of the equivalence surface of the BSM model to be equal to the area of the spherical surface defined by the Bohr radius. We may call the equivalence surface, used in the BSM model, a **Bohr surface**, in order to emphasize the relation to the Bohr radius a_o . Then the right parts of the relation (7.3) could serve as one of the definition parameters of this surface. It is written separately as Eq. (7.3.a).

$$2\pi a_o = \frac{\lambda_c}{\alpha} = const \quad (7.3.a)$$

The parameter $\lambda_c = \lambda_{SPM}$ is valid for free CL space not disturbed by E-field. So it is satisfied outside the the boundary region, that defines the Bohr surface, but we may consider that it begin to be satisfied at the boundary region.

The other definition parameter of the Bohr surface is dictated by the shape of the proton or more accurately said - its proximity electrical field. **The latter possesses a spatial configuration de-**

defined by the proton shape and enclosed inside of the Bohr surface in case of orbiting electron.

In case of single proton without an electron (a positive ion) its electrical field breaks the Bohr surface. In this case the proximity field distribution is still preserved, but outside the Bohr surface the electrical lines are rearranged. So from outside, the proton (ion) appears as a point charge.

Summary:

- **The Bohr surface is an equivalent boundary surface around the proton, with a shape of ellipsoid.**
- **The area of the Bohr surface is equal to the area of the sphere with a radius a_0 .**
- **The spatial orientation of the Bohr surface is defined by the spatial orientation of the proton core**
- **The Bohr surface around the proton is implicitly defined by the CL space parameters λ_{SPM} and α .**
- **In case of orbiting electron the proximity E-field is enclosed inside the Bohr surface.**
- **In case of single proton (or ion) the E-field breaks the Bohr surface. The external E-filed lines in this case are radial to the geometrical centre and simulate a pointlike charge particle.**
- **The shape of the Bohr surface could be modified. This freedom is given by the definition condition Eq. (7.3).**

The position of the Bohr surface around the proton is illustrated by two sections, as shown in Fig. 7.2.

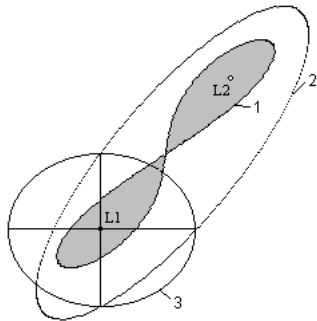


Fig. 7.2

Bohr surface around the proton

- 1 - proton core, 2 - Bohr surface section along the proton length, 3 - Bohr surface section across the proton width, passing through one of the locuses

The quasiplanes of the proton clubs are shown shaded. The two locuses are denoted as L_1 and L_2 .

In order to determine the ellipsoid axes of the Bohr surface we need to know the E-filed lines distribution inside the surface. Their spatial distribution is determined by the twisting characteristic angle θ_w of the external proton shell and the overall shape of the proton. It is more convenient to present a section of equipotential surfaces inside the Bohr surface. The curved E-filed lines should intercept these surfaces at right angle. A possible configuration of the equipotential surfaces in a section passing through one of the locuses is shown in Fig. 7.3.

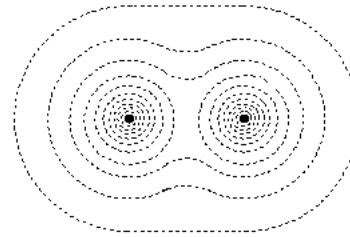


Fig. 7.3

Section of equipotential surfaces inside the Bohr surface

One possible way to determine the Bohr surface parameters is to fit quantum orbits around the proton core, taking into account the equipotential surfaces in all possible sections. In a first gland this is a complicated task. However, we know the shape and length of the proton core and the length of the quantum orbits. Then we could make models of quantum orbits around the proton core with possible shape. One helpful rule in the search for the correct shape is, the following:

- **the motion in the quantum orbit should be characterized with a minimum energy loss.**
This condition is fulfilled, if:
- **the trace of the quantum orbit intercepts the E-filed lines inside the Bohr surface at one and a same angle.**

In the following analysis we will see, that the second condition may not be fulfilled for the whole orbit trace, but for larger or smaller part of the orbit.

The strength of the quantum effect is dependable of this condition. It will become evident, also, that:

- **The quantum effect becomes stronger when the interception angle approaches the twisting angle:** $\theta_w = \theta_{eff}^{lept} = 28.762 \text{ deg}$ (discussed in Chapter 6).

The criterion for the correctness of the quantum orbit shape will be the electron energy, corresponding to the quantum number. The electron energies for the consecutive quantum orbits will correspond to the energy difference between the neighbouring spectral lines in one series. Such model is developed for the Balmer series of the Hydrogen atom. It is presented in §7.8.

7.3 Coulomb force inside the Bohr surface

It is evident, that the distributed positive charge of the proton inside the Bohr surface will provide different interaction conditions between the electron and proton, when the electron is inside of this surface. The inverse square dependence of the Coulomb forces from distance is not any more applicable in such conditions. In order to find the modification of the Coulomb force law inside the Bohr surface we will make analogy with the optical radiation. For this purpose we will take example of a point light source and a point like detector as illustrated in Fig. 7.4. The source and detector, both have the same angle of view. The point source illuminates a screen, the distance from which is fixed and shown as r_{ref} . Let consider that the screen is made of micro corner cube tape, having the property to reflect the rays at same incident angle (the road signs are covered by the same type of tape). This will closely simulate a feature of E-field lines coupling between the point like electron and the distributed E-field lines of the proton. The case *a*, *b*, *c*, corresponds to three different distances of the detector from the screen. The illuminated area is denoted as A_s and the pick up area by detector - as A_d .

In case *a*. the distance between the detector and the screen is larger than r_{ref} . This corresponds to an electron outside the Bohr surface. It can't pick up all the electrical field lines of the proton. The picked up signal is inverse proportional to the quadrature of distance r , normalized to r_{ref} . So this is a classical law of Coulomb forces.

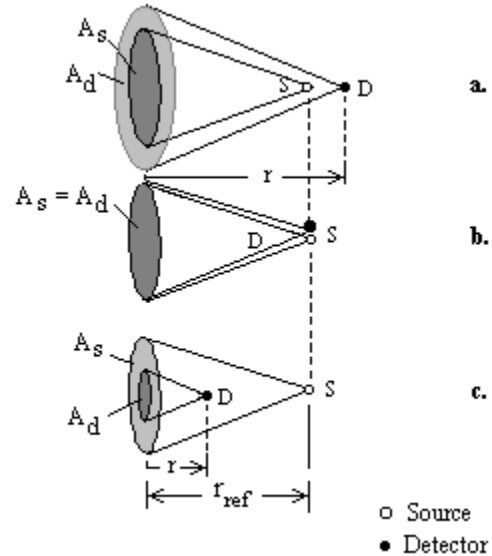


Fig. 7.4

In case **b**. the detector field of view covers exactly the illuminated surface A_s . This corresponds to an electron positioned at the Bohr surface. **All E-field lines of the electrons are connected to all E-field lines of the proton. This is possible if the electron velocity is not very large.**

In case **c**., the picked up signal is proportional to the square of the distance r , referenced to r_{ref} . This dependence is valid only for the range $0 < r \leq r_{ref}$. This case corresponds to an electron inside the Bohr surface. **In such conditions the electron's E-field lines are not able to be interconnected to all E-field lines of the proton, because the proton's E-field lines emanates from a comparatively large proton core envelope surface.**

The above considerations could not be valid at very close distance to the proton core, because the effect of the twisting IG field in the vicinity of the proton and electron external shell will predominate. This may give some increased repulsion in very close distance. Such effect will assure a safe minimal gap between the hardware helical structures of both particle, which is one very important feature for keeping their internal RL(T) structures from destruction (see §6.4.3 Chapter 6).

According to the provided analysis the Coulomb force inside the Bohr surface could be proportional to the term: $\frac{q^2}{4\pi\epsilon_0} r^2$.

Outside of the Bohr surface the atom is neutral, for all series, including the Balmer one. This means, that the whole charge of the proton participates in this term. For the circular sector of orbit around one proton core, however, we may consider, that the electron interacts with half of the E-field lines and, the corresponding force will become proportional to $\frac{q^2}{2\pi\epsilon_0}r^2$.

The shown above term should be normalized to a reference distance, corresponding to r_{ref} in the analogous optical example. It is not difficult to guess, that this reference distance is the Bohr radius, a_0 . It connects the CL space and the electron system parameters: h, ϵ_0, q, m_e , according to Eq. (7.1). Normalising to this distance, we get the equation of Coulomb force between the proton core and the electron in the circular section of the orbit, which is inside the Bohr surface.

$$F_C = \frac{q(q/2)}{4\pi\epsilon_0 a_0^2} \left(\frac{r}{a_0}\right)^2 \tag{7.3.b}$$

where: r - is the distance between the proton core and the electron in the circular part of the orbit.

7.4 Orbital planes for the Hydrogen series.

We will consider here only the orbits, which are related to emission or absorption of photons.

The possible orbits are three dimensional curves and in fact could not define a surface, but we may define an equivalent surface, so the average distance of it from all orbital points (for small time intervals) to be a zero. Then such surface will have a twisted shape, so we may call it **an orbital quasiplane**. One orbital quasiplane is defined by one orbit, but large number of orbits may have a common orbital quasiplane. One spectral series of the Hydrogen atom, for example, corresponds to set of orbits with common orbital quasiplane. **The limit of the series corresponds to the largest orbit of the set, called a boundary orbit.** It will be shown, by the model of the Balmer series, than the number of orbits in the series is limited. The electron kinetic energy, in the boundary orbit can be determined by the limit energy of the corresponding spectral series. Knowing the length of the boundary orbit as a

quantum orbit, the quantum velocity can be determined. **In such way it can be verified, that the boundary orbit is a quantum orbit.** Consequently, we may determine the length of the boundary orbit for any one of the series, using the condition of the quantum orbit.

The equation of the quantum orbit trace length was derived in §3.12.3 (Eq. (3.43.i))

$$L_{qo}(n) = \frac{2\pi a_0}{n} = \frac{\lambda_c}{\alpha n} \tag{3.43.i}$$

where: n is the subharmonic number of the quantum orbit

The positions of the orbits are referenced to the proton core geometry. Then it is more convenient to use the ratio between the quantum orbit trace length and the core length of the proton. For a quantum orbit corresponding to a first harmonic electron velocity, this ratio is:

$$L_{pc}/L_{qo}(1) = 2.042878 \approx 2 \tag{7.4}$$

The ratio (7.4) is very close to a whole number and we may use integers, for convenience, neglecting the small fractions. In §3.12.3 it was mentioned, that subharmonic quantum loops are able to be connected in series, forming in this way a common quantum orbit. We may call such orbit a **serial quantum orbit**. Table 7.1 shows the ratio calculated for different subharmonic numbers, n , and for both types of orbits: single and serial. The ratio is rounded to integer or close fractional numbers for convenience.

Possible quantum orbits according to the approximate ratio $L_{pc}/L_{qo}(n)$ Table 7.1

n	single quantum orbit	serial quantum orbit comprising:				
		2 loops	3 loops	4 loops	5 loops	6 loops
1	2					
2	1	2	3	4		
3	1/3	2/3	1	4/3	5/3	2
4	1/4	2/4	3/4	1	5/4	6/4
5	1/5	2/5	3/5	4/5	1	6/5
6	1/6	2/6	3/6	4/6	5/6	1

Different subharmonic number means a different quantum velocity of the electron. The selection rule for a proper orbit is additionally influenced by the IG forces. For this reason a mod-

el involving the balance between all forces is necessary. Such model is developed for the Balmer series. Based on this model and additional considerations of orbits in other atoms, the orbital quasiplanes of Lyman and Balmer series are identified with a high degree of confidence. The boundary orbit for the Lyman series correspond to ratio 2, while for the Balmer series - to ratio 1 (according to Table 7.1).

Figure 7.5 shows the position of the boundary orbits of the Lyman and Balmer series referenced to the proton shape. They define also the orbital quasiplanes.

The boundary orbits for the higher order Hydrogen series may occupy the same orbit as the Balmer or the Lyman series. Below the boundary orbit however, the higher order series may have serial orbits (the latter option is not enough investigated by BSM). (For atoms with higher Z number, the Lyman quasiplane becomes less accessible and the Bohr surface becomes distorted).

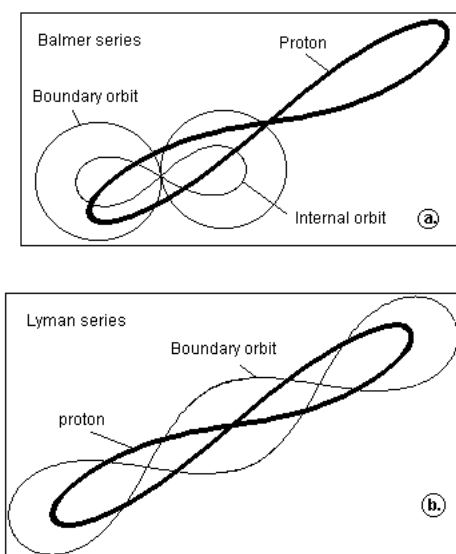


Fig. 7.5

We see that the orbital quasiplanes of Lyman and Balmer series are quite distinguishable one from another. The orbital quasiplane determines the positions of many quantum orbits, but the boundary orbit is the largest one. It is reasonable to accept that the boundary orbits of all possible quasiplanes are inside the Bohr surface, so in all this cases the Hydrogen atom appears as a neutral. The electron may change also the orbital quasi-

plane if getting or losing a large amount of energy due to some elastic collision of the Hydrogen with another molecule. The probability of quasiplane change in a spontaneous emission however is much lower than changing of the quantum orbit in the same orbital quasiplane. We may consider, that in the process of ionization, the lost electron has been in one of the possible quasiplane. It is reasonable to consider that atoms with $Z > 1$ may also have conditions for different orbital quasiplanes as the Hydrogen. However, the possible quasiplanes are dependent of the proton and neutron arrangement in the nucleus, as this will be shown in Chapter 8 and the Atlas of the atomic nuclear structures. In any case, however, the ionization is possible.

Figure 7.6 illustrates the possible shape of boundary orbits for higher hydrogen series.

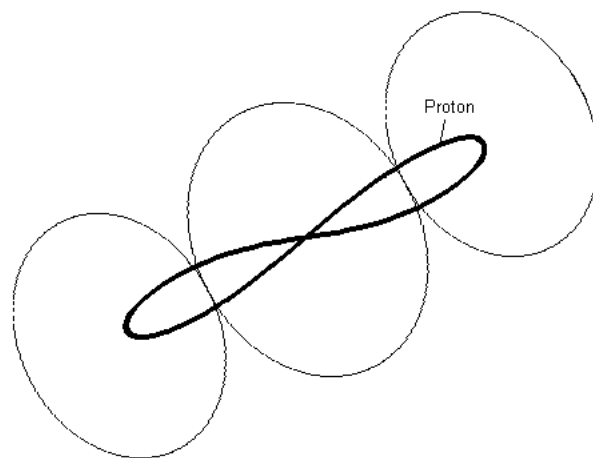


Fig. 7.6

Possible shape of boundary orbits for the Hydrogen series of higher orders

The existence of more than one boundary orbits, could be explained also by the flexibility of E-field refurbishment that may modify the shape of the Bohr surface. We may assume that the Bohr surface have a constant area of $4\pi a_0^2$ but a flexible shape, depending of the working orbits and the interconnection of the proton to other protons in the atomic nucleus. Below the Bohr surface, the E-field possesses a spatial structure, confined to the proton shape and the characteristic twisting angle θ_w of the E-field line emerging from the proton's core. The circulated electron in the orbit intercepts most of the E-field lines at constant angle. In the Bohr surface region this condition (intercepting E-

filed line angle) is disturbed. In the same time the electron possesses a finite momentum even at the Bohr surface (this is shown later in the Balmer model). Consequently, the electron is able to escape from the boundary orbit, if the momentum is large enough.

Below the boundary orbits are all orbits contributing to the series, terminated with the ground state orbit.

- **According to BSM, every series has its own ground state orbit, which is the shortest one.**

This conclusion will be demonstrated for the Balmer model.

The quantum conditions defining the stable orbits are discussed below.

We may use the term **orbital** for all orbits in one series. Although we have to keep in mind that it does not correspond to the term orbitals used in the quantum mechanics (where they are defined by the wave function). We see also that the orbital quasiplanes are curved but open surfaces. The electron transitions between any two orbits are in one orbital quasiplane. The passing of the electron from one to another orbital quasiplane requires special conditions and is less probable.

From the considerations presented so far and from the further analysis we can formulate the following physical rules for the orbits:

- **The orbits for all line series are inside the Bohr surface**
- **Any orbital quasiplane, related with photon emission or absorption, intercepts one or two proton clubs**
- **The boundary orbits approach the zero level potential**

7.5 Effect of the orbiting electron on the atomic motion in CL space.

It is evident that the electron trajectories reside in the orbital quasiplane. The latter is an open surface and could not affect the static pressure of the CL space exercised on the protons and neutrons, and consequently - the atomic mass. Although the orbital momentums of the electrons could affect the atomic motion in the lattice space, causing a spin rotation. For a simple physical analogy the orbital's twisted quasiplanes behaves as a

fins of mechanical object, causing a rotation of this object when moving in a fluid.

Let considering a neutral Hydrogen atom, moving with constant velocity. The most probable orbit is the ground state. The electron has its own momentum that defines the orbital momentum. But in order to keep this momentum in the Hydrogen motion, the interaction with the lattice should be minimal. Then the Hydrogen has to rotate with some confined spin because the orbital shape is twisted. In result of this motion, the electron could make transitions between very close orbitals. So it may pump the CL space with very low energy, that could be periodically emitted as a low energy photon. The input energy for such emission may come from the equalization of the zero point energy of the CL space. Such radiation will contribute to the Cosmic Microwave Background, corresponding to the temperature of 2.72 K. It might be contributed not only by the Hydrogen atoms and molecules, but from other atoms and molecules, as well. The motion behaviour of such atom or molecule will simulate a "flying bird" but with simultaneous rotational motion.

From the detailed atomic nuclear structure discussed in Chapter 8, we will see that many aspects of Hydrogen orbital structure are preserved in the atoms with higher Z number.

Summary

- **The orbital momentum affects the proton confined motion in CL space**

7.6 Quantum motion of the electron in electrical field. Quasishrunk CL space.

The ionization energy of the Hydrogen atom is 13.6 eV corresponding to the optimal velocity of the electron. Consequently, all orbitals velocities are of suboptimal type. The quantum motion for such velocities was analysed in §3.9. The analysis, was provided for CL space without external electrical field. In Hydrogen atom, however, all orbits are inside the Bohr surface, where the electrical field has a specific spatial configuration, defined by the proximity field of the proton and the proximity locked field of the neutrons. Let denote a CL space without external electrical and magnetic field (other than the electron own fields) as a **free CL space** and the CL space with an external E-filed - as a **E-**

field CL space. Then we may distinguish two cases of the electron confined motion:

- (a) electron motion in a **free CL space**
- (b) electron motion in a **E-field CL space**

The case (a) was analysed in Chapter 3. The quantum motion of the electron is defined by the CL space parameters. Between them are the Compton wavelength, λ_{SPM} , which is defined by the SPM frequency and the light velocity. For a free CL space we have $v_{SPM} = v_c = v_e$, where, v_e is the first proper frequency of the electron system (electron shell - positron). **In the end of §2.11.2.2 it was discussed, that the stationary EQ of the CL nodes may possess higher resonance frequency, than the MQ node.** This automatically means that they will have a higher SPM frequency (a higher SPM frequency for CL space with not changed node distance means a shorter SPM cycle and a shorter propagated SPM phase, i. e. **a shorter SPM wavelength λ_{SPM}'** in comparison to the free CL space).

$$v_{SPM}' > v_{SPM} \quad \text{or} \quad \lambda_{SPM}' < \lambda_{SPM} \quad (7.5)$$

where: the prime sign denotes the corresponding parameter in the E-field CL space.

It is apparent from Fig. 7.5 that the Balmer quasiplane is much less twisted than the Lyman one. This makes Balmer orbits more convenient for analysis. The electron orbits for Balmer series occupy the range between the proton core and the boundary orbit. Around the proton core, their traces tend to follow the equipotential curves as illustrated in Fig. 7.3.

According to the derived rule for the interception angle between orbital trace and E-field lines (see §7.22), it follows, that there is a tendency of keeping a constant value of this angle with variations within a limited angular range. Consequently, the condition (7.5) will be more or less valid for the motion in any one orbit below the boundary one. In the same time, the electron proper frequency v_e is unchanged, because the electron system possesses own internal energy. While the E-field does not affect the CL space node distance, it affects the SPM wavelength, making it shorter. But the SPM wavelength is a specific quantum parameter of the CL space influencing the light propagation and the electron quantum motion. So if the electron velocity is estimated by the node distance, the quantum velocity appears smaller, the follow-

ing the shorter λ_{SPM}' . In the Balmer orbits model, presented in the next paragraph, it is accepted, that in the E-field CL space inside the Bohr surface, λ_{SPM}' changes linearly with the radius of the circular part of the orbit. In this case, the obtained results of the model are optimal. The figure of merit is the shape of the calculated energies corresponding to the Balmer series spectra. The linear dependence may be a result not only of the proton E-field configuration below the Bohr surface, but also of the magnetic field lines caused by the electron motion and oscillation.

The reduced value (shrinkage) of λ_{SPM}' and the orbital length dependence on it gives a possibility the space below the boundary orbit to contain a larger number of orbits.

The shrinkage of the λ_{SPM} inside the Bohr surface complicates the analysis, because the quantum scale becomes different. **In order to solve this problem, we may consider, that the quantum space is quasishrunk.** The term quasi is used, because the CL node distance is not changed and the proton's dimensions - also, but the shrinkage is valid only for the quantum conditions. In order to keep this into account, we have to translate the necessary parameters to the scale of the quasishrunk quantum space, i. e. to λ_{SPM}' (the prime is used to denote the shrunk value of the parameter). The field forces and inertial momentum also has to be referenced to this scale. **In such case, the inertial mass of the electron referenced to λ_{SPM}' scale will be affected.** When analysing the motion in the circular part of the orbit, **the apparent inertial mass will appear larger**, because the electron intercepts smaller number of nodes per λ_{SPM}' . We may test a linear or a quadratic dependence of the apparent inertial mass in function of orbit length (or distance from the proton core). The quadratic dependence, which is a symmetrical function of the Coulomb force inside the Bohr surface provides better results in the Balmer model.

The quasishrunk quantum space affects not only the electron motion but the quantum waves as well. The internal space inside the Bohr surface behaves as an optical media with gradual index change. In such way, it affects the propagation of the quantum waves in the X-ray range. This behaviour is discussed in Chapter 8. Consequently, we may accept that the space is characterised with a

gradual refractive index. This refractive index is valid only for electron motion at proper orbits and for incident quantum wave falling at proper incident angle.

The static pressure is from all direction forces exercised on the FOHSs, valid also for the electron. According to this formulation, the static pressure in E-field CL space should not be changed, because the average node distance is unchanged. Then the electron system parameters are preserved. This is valid also for the fine structure constant, estimated as a ratio between the tangential and axial velocity of the electron.

Summary:

- **In E-field CL space, the SPM wavelength along the equipotential curves is reduced**
- **The electron performing a quantum motion in equipotential curve exhibits increased apparent inertial mass, if referencing its motion to the quasishrunk quantum space**
- **The refractive index of the quantum quasishrunk space is valid for electron motion at proper orbit and for incident quantum waves falling at proper angle in respect to the proton club quasiplane.**

7.7 Quantum orbit conditions for orbits inside the Bohr surface.

7.7.1 Quantum conditions, related to the orbital length

The quantum loop was defined in §3.12.2 based on the matching the energy conditions between the Bohr model and the BSM model of quantum orbits. **The quantum loop is a closed loop trajectory of the electron moving with confined velocity. The loop trajectory length is defined by the condition of whole number of carrier oscillations.**

The number of electron's full rotations in the quantum loop of electron with first harmonic quantum velocity (13.6 eV) was define in Chapter 3 by the equation

$$\frac{2\pi a_o}{s_e} = \frac{\lambda_c}{\alpha s_e} = 18778.362 \quad [(3.43.h)]$$

We see, that the value is very close to 18778.333(3). The difference is only (1.53E-4)% and might be a result of small error in the experi-

mental estimation of the fine structure constant α . Having in mind that the second proper frequency of the electron system (the internal positron - central core frequency) is 3 time higher we see that for one quantum loop it make a whole number of cycles:

$$18778.333(3) \times 3 = 56335 \quad \text{cycles of positron-core}$$

The obtained phase repetition conditions could be considered as a shortest orbital time condition, valid for a first harmonic quantum orbit.

The next condition for a phase repetition of both proper frequencies is for 3 orbital cycles. It will contain 56335 full electron rotations or 169005 cycles of the internal "positron-central core" system. The theoretical expression of this condition is:

$$\frac{3\lambda_c}{\alpha s_e} \quad \text{where: } s_e \text{ is the electron helical step}$$

Let consider now the same effect for a second harmonic quantum orbit, that is valid for the Balmer series. The axial velocity and rotational rate of the electron are twice slower, but the orbit is twice shorter than the first harmonic orbit. Therefore, the time of one orbital cycle is the same and the electron system possesses one and a same number of cycles for its two proper frequencies. **This condition is valid also for larger subharmonic electron motions but only for single quantum loop.** For the higher subharmonic numbers in Hydrogen, however, single quantum loops does not fit to the proton structure. Consequently the orbits of the higher order series (3rd, 4rd, 5th, 6th) are composed of serial quantum loops.

The condition of the phase repetition is only the necessary but not enough condition related to the finite orbital time (a lifetime of exited state). A second condition causing the dropping to lower orbit is from the mismatch between two short magnetic line conditions, described later in §7.7.2.

The result for a phase repetition of oscillating electron was derived for a free CL space, whose conditions are also valid for the boundary range of the Bohr surface. If the λ_{SPM} below the Bohr surface gradually change, as discussed in the previous paragraph, the above condition (56335 full cycle) is still preserved. It is only necessary the cosine between the negative core oscillation, and the E-field lines of the proton to have enough small dispersion around one mean value defined by the orbital position. Keeping in mind, that the E-field are subordi-

nated by the angle θ_w , but are enclosed in the internal volume enclosed by the Bohr surface, it is apparent that the condition for quantum orbits could be satisfied for a spatial range inside that surface.

Consequently the quantum orbit conditions may be valid for large number of orbits, below the boundary one.

It will become evident from the analysis later, that the above mentioned conditions are valid for all the orbits and orbital transitions that provides line series of the Hydrogen atom.

If the above conclusion is correct, an additional quantum condition is necessary in order to provide an individual orbit separation, corresponding to the different quantum energy levels.

- **The condition for orbit separation is provided by the magnetic line, aligned with the spin axis of the orbiting electron.**
- **The above condition is contributed by the spin rotation of the orbiting electron.**

When the electron provides a repeatable motion in a quantum loop, its spin rotation is an important attribute of the motion. The velocity vector of the rotating electron shell is normal to the orbital trace, so the magnetic lines from the spin appear parallel to the orbital trajectory. Having in mind the radial E-field distribution (see Fig. 3.6, Chapter 3) and the quantum magnetic radius, we may distinguish **two separate bundles of magnetic lines from the spinning electron: peripheral and axial.** The peripheral one is related to the quantum magnetic radius and will have a shape of hollow tube around the electron shell. The rotating electron provides a large concentration of magnetic field lines passing through the axis of its rotation. This will cause deterioration of the external E-field of the proton in a narrow zone centered around the electron orbital trace. **Consequently, we may consider that the axially aligned field of of the moving electron creates a path with MQs, having the same SPM frequency as the CL space outside of the Bohr surface, where the E-field is missing.** In the same time the magnetic lines in the peripheral field occupy a larger volume and do not lead to disturbance of the proton E-field. As a result of this analysis, we arrive to two important conclusions:

- **The peripheral magnetic lines from the spinning electron interact with the E-field CL space created by the proton.**
- **The axial magnetic lines occupy a small volume space, while the proton E-field in this space is deteriorated. The CL nodes in this space are of MQ type with a same SPM frequency as the external free CL space.**
- **The λ_{SPM} in the peripheral space along the orbital trajectory is shrunk, while in the axial space it is the same as in the free CL space.**

Having in mind, that the magnetic line is a loop of zero order SPM waves, it is close to the mind, that its length should contain a whole number of λ_{SPM} . For large size of magnetic loops, this condition is quite easy to be satisfied. The same is not true for the size of the electron orbits in atoms. The whole number of λ_{SPM} is enough strong quantum condition in order to define the stability conditions for an individual orbit. Therefore, this could be regarded as a quantum condition related to the magnetic lines. We may call this quantum condition a **short magnetic line condition.**

- **The short magnetic line condition, provides quantum conditions for individual orbit separation in the series. It is based on the assumption, that the length of the magnetic line loop should contain a whole number of λ_{SPM} .**
- **The short magnetic line condition is valid for the peripheral and axial magnetic lines, created by the spinning electron.**

It is evident, that the individual orbits corresponding to one series fulfil simultaneously two quantum conditions: the quantum loop condition and the short magnetic line condition. In the same time the short magnetic line condition is valid for the peripheral and axial magnetic lines from the spinning electron. Analysing the Balmer model we will see, that **the first one determines the orbits separation, while the second one defines the finite time of the electron on a particular orbit.**

Figure 7.7 illustrates the short axial magnetic line condition for one particular orbit in Balmer series.

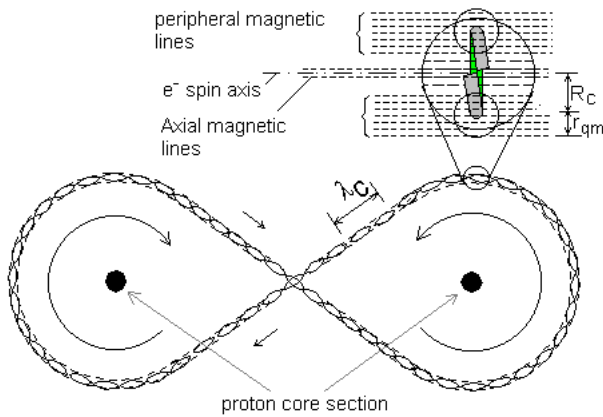


Fig. 7.7

Stable orbit defined by the short magnetic line condition. The peripheral and axial magnetic lines are from the electron spin rotation

The shown sinusoids along the orbital trace indicates the whole number of longitudinal λ_{SPM}' , in a E-field CL space. They fulfil the short magnetic line condition for the peripheral magnetic lines, which are induced by the spinning electron. This condition defines the orbit separation in the Balmer series. A momentary position of the orbiting electron and its exploding view are shown in the same figure. The spatial configuration and density of the peripheral magnetic lines are determined by the quantum magnetic radius r_{mq} . The r_{mq} radius for Balmer series is defined by the second subharmonic quantum velocity. While the short magnetic line condition from the peripheral lines defines the orbit separation, the same condition for the axial lines defines the total time duration of the individual orbit. This will become evident by the analysis of Balmer model.

The shape of the orbit shown in Fig. 7.7 is idealised. The real orbit could be distinguishable in a way, that the section around the proton core may not be a perfect circular and the sections between the circular parts may not be straight lines. Despite of the accepted simplification, the adopted shapes of the orbits lead to consistent results of the model.

7.7.3 Summary for quantum orbits:

- **The quantum loop condition is valid for all orbits corresponding to the energy levels of one spectral series**

- **The short magnetic line quantum condition provides individual orbit separation in the series**
- **The orbiting electron comply simultaneously the both quantum conditions**
- **The separation of the quantum orbit into a number of orbits is a result of λ_{SPM}' change in function of the distance from the proton core, in the E-field CL space inside the Bohr surface**
- **The phase repetition time of the two proper frequencies of the electron is characterized by two time cycles corresponding to the whole number of the particular cycles.**

7.7.4. Electron orbits contributing to the sharp spectral lines in the series

The spectral series of the Hydrogen atom are measured with high accuracy. It is well known feature, that when approaching the energy limit for every one of the series, the lines become less distinguishable and finally converts to a continuum. The quantum mechanical model gives explanation of this effect by accepting infinite number of closed spaced levels. The BSM model, however, leads to a different conclusion:

- **The obtained continuum is not from infinite number of levels, but from deteriorated quantum conditions. Such conditions cause some energy variation of the emitted quantum waves that is detected as widen spectral line shape.**

Let take for example the Balmer series. Not all orbits below the boundary one contribute to the sharp spectral lines. There is a range below the boundary orbit, where the quantum orbit conditions in E-field CL space are not well fulfilled. This is illustrated by Fig. 7.9, where all shown dimensions are in scale.

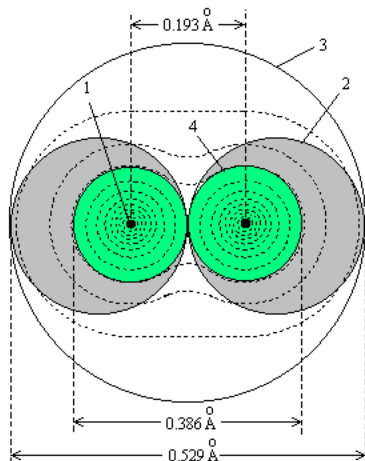


Fig. 7.9

Boundary and limit orbits in the Balmer orbital quasiplane: 1 - proton core; 2 and 3 - boundary orbits, 4 - limit orbit. The region associated with the for sharp line series is shown by green colour (internal circles) while the region with smeared lines with a grey colour (external circles)

Two possible boundary orbits are shown: 2 and 3. The both have one and a same length, but the orbit 3 is more probable for the escaping electron, while the orbit 2 still passes through the proton club. The space inside the limit orbit 4 (green area), is occupied by orbits contributing the Balmer series spectral lines. In this region large section of orbital trace coincides or follows the equipotential curves. (The E-field interception angle of the equipotential surfaces inside the Bohr surface are not exactly at 90° due to the characteristic twisting angle θ_w). In the region between the limit and boundary orbit (grey area) the mentioned above condition is not fulfilled and the quantum orbital conditions are deteriorated. This causes an increase of the line width and appearance of continuum.

Figure 7.10 shows a shape of orbit from Balmer series in the region corresponding to the sharp spectral lines, together with the E-filed lines around the proton core. The E-filed lines are shown normal in the circular regions around the proton core, for drawing convenience, but in the real case the angle is not exactly $\pi/2$, due to the twisting angle θ_w .

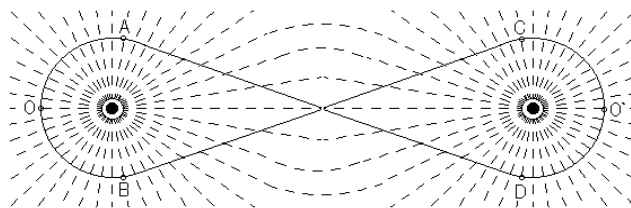


Fig. 7.10

Idealized orbital shape from Balmer series in the region corresponding to sharp spectral lines.

7.8 Model of the Balmer series

Note: This is an example model with mostly qualitative output results. The quantitative results may not be considered as final, because the model have more than one adjustable parameters.

7.8.1 Purpose and general considerations

The purpose of the model is to provide some verification about the correctness of the quantum orbits concept, developed in the previous paragraphs. The model is approximated, because it contains some unknown or partially known parameters, so there are more than one adjustable parameters.

The known parameters are:

- proton core and proton width
- shape and length of the boundary orbit
- shape and length of the limit orbit
- approximate shape and length of the ground state orbit
- both quantum conditions at the boundary orbit

The unknown parameter is:

- the inverse power degree of the leaking (in CL space) IG forces between the proton and electron structures

Partially unknown parameters:

- the parameters of the quantum quasi-shrunk space inside the Bohr surface

The **figure of merit** is the correct shape of the curve presenting the calculated by the model energy levels of the Balmer series.

It is evident, that the attraction IG force between the proton core and the electron affects the electron motion. These forces appears as leakage IG forces through CL space, so they are not any more proportional to the inverse cub of the distance

(like in a pure void space). The modified IG law through CL space should appear in higher inverse order. (see Fig. 2.8.b and the discussion of feature 7 in §2.6.1). In our case we will simulate the IG low through CL space by using the Newtonian mass of electron as unit mass and the Newtonian gravitational constant. The attraction IG force is expected to appear with a large inverse power than 3, because the leaking IG field in CL space falls faster with the distance, than the IG field in pure empty space. Applying the defined above figure of merit we may obtain the degree of the IG law valid for the distance range limited by the Bohr surface.

The determination of the parameters of the quantum quasishrunk space is more controversial. The space inside the Bohr surface is characterised by:

- two different regions, as shown in Fig. 7.8, the region of spectral series and the region of the continuum
- the region of spectral line could be divided into two zones: two zones of the circular orbit trace around the proton core and one middle zone between them.

We may simplify the problem if deriving parameters from the orbit lengths and the proton dimensions. For this reason we use idealised shape of the orbits, estimating the quantum quasishrunk factors for the orbits which lengths are known.

In order to express the orbital dependence on λ_{SPM}' , it is necessary to introduce a quantum quasishrink factor. If assuming a linear dependence (that will be confirmed by the results) it is more convenient to define a quasishrink ratio, k_{qs} . It is equivalent to consider, that k_{qs} is defined as a ratio between the λ_{SPM} at Bohr surface (corresponding to a free CL space) and λ_{SPM}' at the Balmer Ground State (GS) orbit. Once determined, we may reference the quasishrunk ratio to the Bohr surface, where all the CL space and electron parameters are defined, by the physical constants. The reciprocal of the quasishrink ratio is equal to the gradient refractive index. The existence of this index around the proton club will be discussed in Chapter 8 in connection with X-ray properties of the solids.

- **The quantum quasishrink refractive index is reciprocal to the quasishrink ratio. It could be denoted as n_{qs}**

$$n_{qs} = 1/k_{qs}$$

The Bohr surface could not be considered as a surface with a stable shape. The electron, when orbiting in different quasiplanes, may cause a different deformation of the Bohr surface. The physical constants, like h , q , m_e , v_c are valid for the space outside of the Bohr surface. In order to use them we have to translate some of the Balmer model parameters to the Bohr surface. In many cases it is more convenient to use the Bohr radius or the length of the Bohr orbit.

7.8.1.A. Approximative determination of the quasishrink ratio for Balmer series

The quantum orbits contributed to the Balmer series lie on the Balmer quasiplane (now considered as plane for a simplicity) and occupy the internal circle regions, shown in Fig. 9.7. It is reasonable to accept a linear dependence of the quasishrunk SPM wavelength λ_{SPM}' in function of the distance from the proton core. Then the approximate value of the quasishrink factor could be obtained by the ratio between the Bohr orbit length $2\pi a_o$ and the shortest orbit. The shortest orbits is the ground state (GS) orbit. One factor restricting the orbital length is the finite distance between the two proton cores in the Balmer orbital plane. Having in mind the requirement for safety margin between closely spaced FOHSs discussed in Chapter 6, it is reasonable to accept the magnetic radius of the electron and proton as a second factor.

. This condition is illustrated in Fig. 7.11, where r_{eq} is the magnetic equivalent radius of the electron for the second subharmonic (see §3.11 and Table 3.3).

The magnetic radius for the second subharmonic was given in Table 3.3: $r_{eq} = 2.109 \times 10^{-12}$. Then

$$r_o = (R_c + r_p) + (R_c + r_{eq}) = 9.89 \times 10^{-13} \text{ m}$$

The length of the idealized orbits in the orbital range: GS orbit - limit orbit, is given by the Eq. (7.6):

$$L_{orb} = 2[d\sqrt{1 - 4r^2/d^2} + r(\pi + 2\text{asin}(2r/d))] \quad (7.6)$$

where: r - is the orbit distance in the circular part from the centre of the proton core; d - is equal to the proton width (given by Eq. 6.77)

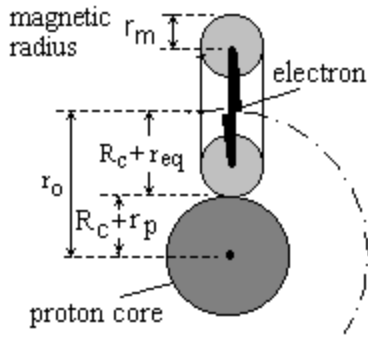


Fig 7.11

Definition conditions for r_o , corresponding to the Balmer GS orbit

The Balmer GS orbit length, obtained by the conditions of finite magnetic radius is 0.45018 Å (1 Angstrom = 10^{-10} m). The length of the Balmer boundary orbit is: $2\pi a_o = 3.3249187 \times 10^{-10}$ (m)

Then the approximative mean value of the quasishrink ratio, k_{qs} , could be defined as ratio between both orbits:

$$k_{qs} = 7.385 \quad (7.7)$$

The quasishrink ratio gives a possibility to define the change of $\lambda_{SPM'}$ in the Balmer orbital plane as a function of distance from the proton core. This is used in the next paragraph.

7.8.2 Concept of the model

The concept of the model is based on the energy calculation of the possible quantum orbits, related to the spectral lines of the Balmer series (without the continuum near the limit). These orbits cover the range between the Balmer Ground State (GS) orbit and the limit orbit (denoted as 4 in Fig. 7.8). The orbit positions are illustrated by Fig. 7.13. Their shapes are idealized for convenience. Every orbit contains two circular sectors around the proton cores connected with tangent lines, passing through the proton club locus. The trace length of such geometrically simplified orbits is given by Eq. (7.6).

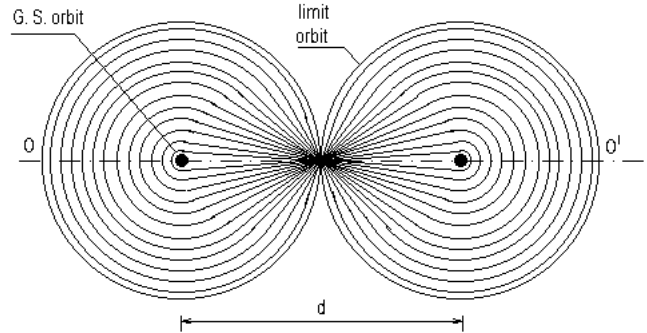


Fig. 7.13

Idealized orbits for Balmer series

Complying the short magnetic line quantum condition for the peripheral magnetic lines related with the quantum magnetic radius of the electron, the length between the neighbouring orbits will differ exactly by $\lambda_{SPM'}$.

The energy level of all orbits can be estimated by applying a balance of forces for the motion of the electron in the circular sector of the orbit. The electron velocity in any orbit depends on the intrinsic gravitational force, F_{IG} , the internal Coulomb force, F_C , and the inertial force from the apparent inertial mass. The balance of forces for this region is given by Eq. (7.8), from where the electron velocity is expressed by Eq. (7.9).

$$F_C + F_{IG} = m \frac{v^2}{r} \quad (7.8)$$

$$v = \sqrt{\frac{r}{m}(F_C + F_{IG})} \quad (7.9)$$

The Coulomb forces inside of the Bohr surface has been presented by Eq. (7.3.b) where the argument r is counted from the radius of the GS orbit. In order to use later the quantum numbers as adopted by the Quantum Mechanics, we will use a shifting parameter r_{GS} . From geometrical considerations we may consider that when the electron circles around one proton club it interacts only with the half of the proton charge. Using Eq. (7.3.b) and applying these considerations we arrive to Eq. (7.10) for the Coulomb force inside the Bohr surface.

$$F_C = \frac{q(q/2)}{4\pi\epsilon_0 a_o^2} \left(\frac{r - r_{GS}}{a_o - r_{GS}} \right)^2 \quad (7.10)$$

where: r - is a running parameter - the distance of the orbit interception point with OO' axes from the proton core centre (absolute units)

r_{GS} - is the distance of the Balmer G.S orbit interception point with axes OO' from the proton core centre (see Fig 7.9). In order to satisfy the quantum condition, r_{GS} is very close to r_o , but at distance not larger than one λ_{SPM}' .

$(q/2)$ - is a proton core charge portion affecting the electron motion at point O.

In order to apply the quantum condition for orbit separation, we have to use λ_{SPM}' , but it depends of the argument r . For this reason it is more convenient, to accept a constant λ_{SPM} , referenced to the distance of the boundary orbit and to correct the argument in the expressions of the IG force, the Coulomb force and the inertial force. It is equivalent to work in units of quantum quasishrink space. Then we can use directly the quantum number of the orbit.

The **inertial mass law in a quasishrunk space** is a controversial problem, not investigated enough. It was discussed in §7.6. A set of laws are tested in the model. The best results are obtained for a square law dependence, when the curve shape is a mirror image of Coulomb law inside the Bohr surface (the mirror axis is parallel to the horizontal axis). So the electron inertial mass dependence on the distance in the quasishrink space is simulated by the Eq. (7.11).

$$m = m_e n_i^2 - m_e (n_i^2 - 1) \left(\frac{r - r_{GS}}{a_o - r_{GS}} \right)^2 \quad (7.11)$$

where: n_i is the quasishrink index of the zone around the proton core, assuming that λ_{SPM}' is a linear function of the argument r .

The simulation of the IG forces through the CL space was discussed in Chapter 2 §2.6, feature 7. The IG forces between the proton core and the electron are presented as a higher degree inverse power law between a mass point and a mass bar. The Newtonian mass of the electron is used as a mass point, while the proton core - as a bar of such mass points. One single coil of the external positive shell of the proton core contains approximately the same intrinsic mass as the electron. Then the mass of the proton core can be expressed as number of N electron masses. Then the differential gravitational field, dg , is given by the Eq. (7.12)

$$dg = \frac{GM}{L((r^2 + x^2)^{0.5})^P} \cos(\alpha) dx = \frac{GNm}{L((r^2 + x^2)^{0.5})^P} \frac{r}{(r^2 + x^2)^{0.5}} dx \quad (7.12)$$

where: L is the length of the mass bar; M is its intrinsic mass; m - is the point mass for which g is estimated; N is the number of mass points, from which the bar is consisted, r - is a distance; x - is a running parameter for integration; and P is the degree of the inverse power law.

The integration on x gives the intrinsic gravitational field, from which the gravitational force is expressed. The tuning of the model requires precise adjusting of the power degree. For this reason a numerical integration is preferable.

The bar length is proportional to the number of mass point. So it is more convenient to replace N by a length of the bar, L , in order to have one and a same units of distance. The parameter L could be expressed as a fraction of L_{pc} and the model could be tested for different L . Then we arrive to the expression of the IG force that leaks through CL space in the range between the electron and nearby proton core.

$$F_{IG} = \frac{2rGm^2}{L} \int_0^{L/2} \frac{1}{(r^2 + x^2)^P} dx \quad (7.13)$$

From the Eq. (7.13) we see that the factor p after the integration will corresponds to a power law of degree P , according to the expression (7.14)

$$P = \frac{p - 0.5}{0.5} \quad (7.14)$$

Replacing the value of F_C and F_{IG} in Eq. (7.8) we get the velocity in function of distance r . In all equations the converted mass is included by its expression given by Eq. (7.11). Now we need to connect the forces balance condition with the quantum condition of the orbit separation based on the whole number of λ_{SPM}' for any orbit length. For this reason the Mathcad program `st_w_qn.mcd` is used. The length of the orbit in function of the distance r is determined by Eq. (7.6). In this point of the model, we have two options for applying the short magnetic line condition (the magnetic lines induced by the spinning electron):

- (a) - for the peripheral magnetic lines

(b) - for the axial magnetic lines

For case (a), assuming a linear dependence of λ_{SPM}' from the radius r in the circular zone and referencing to the $\lambda_{SPM} = \lambda_c$ for the boundary orbit, we have:

$$\lambda_{SPM}' = \lambda_c \left[1 - \left(1 - \frac{1}{k_{qs}} \right) \frac{a_o - r}{a_o - r_o} \right] \quad (7.15)$$

The curvature of the calculated energy levels from the model output is very dependable of the quasishrink ratio k_{qs} . Its value estimated in the previous paragraph is 7.385, but the model, shows better results with a value $k_{qs} = 7.728$. Taking into account the very approximative method for estimation of this parameter such small deviation could be acceptable.

For case (b) the SPM wavelength is a constant and is a same as for the external CL space λ_{SPM} .

The case (a) and (b) separates the model into two similar branches. Let following the case (a), as it is related with the quantum orbit separation.

The length of the quantum orbit expressed as a whole number of λ_{SPM}' is given by Eq. (7.16).

$$L_q = (k_{min} - 2 + n) \lambda_{SPM}' \quad (7.16)$$

where: k_{min} is the number of wavelengths for the nearest to the core orbit, but not closer than r_o ; **n is a principal quantum number; the factor 2 is for matching the orbit number to the quantum mechanical principal quantum number for Balmer series.**

Substituting (7.16) in (7.15) and equating the result with the Eq. (7.6), we arrive to Eq. (7.17).

$$2 \left[d \sqrt{1 - 4 \frac{r^2}{d^2}} + r \left(\pi + 2 \sin \left(2 \frac{r}{d} \right) \right) \right] = L_q(n) \lambda_{SPM}'(r) \quad (7.17)$$

Giving consecutive numbers of n starting from 2, the corresponding distance r is determined and discrete value function $r(n)$ is obtained. The function $r(n)$ is fitted to a curve.

$$r(n) = a + bn^c \quad (7.18)$$

where: $a = 0.00396279$; $b = 0.0051841$; $c = 0.7947166$

The fitting results are shown in Fig. 7.14.

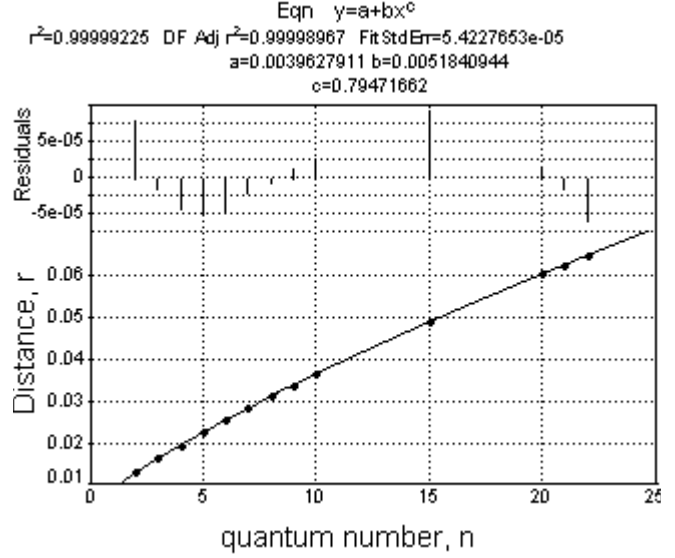


Fig. 7.14

Substituting the argument $r(n)$ in all terms of the Eq. 7.9, **we obtain the electron velocity in function of the quantum number.** The plotted curve of this discrete value function is shown in Fig. 7.15.

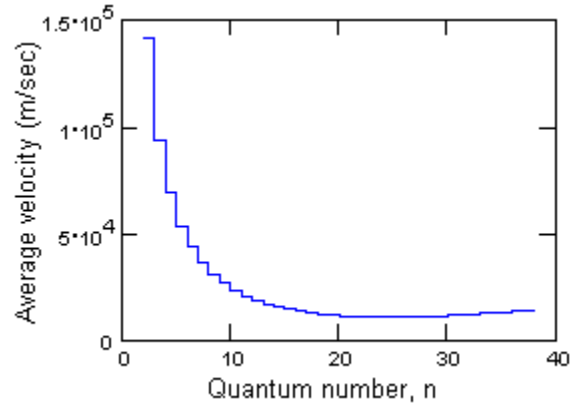


Fig. 7.15

Orbital electron velocity in function of the quantum number

All spectral lines of the Balmer series are between 3.4 eV and 0 eV. The velocity in the GS orbit with $n = 2$ corresponds to 3.4 eV, while the velocity of the limit orbit with $n = 39$ corresponds to 0 eV. The plot in Fig. 7.15 shows, that the velocity is decreasing with the quantum number for the range $2 < n < 26$ and then slightly increased for $n > 26$. We may call the first region a **region of velocity inversion**.

The velocity curve is referenced to the GS velocity. This velocity is determined as a second subharmonic velocity corrected by the quasishrink index n_{qs} :

$$V(2) = \frac{\alpha c}{2n_{qs}} \quad (7.19)$$

Where the quasishrink index is inverse proportional to the quasishrink ratio k_{qs} .

The model velocity equation (7.9) should give the same value for $n = 2$ as Eq. (7.18). For this reason only the parameter p in Eq. (7.11) is tuned. The corresponding degree of the inverse power law of IG forces, is obtained by Eq. (7.14). The plot of IG forces together with the plot of the Coulomb forces are both shown in Fig. 7.16.

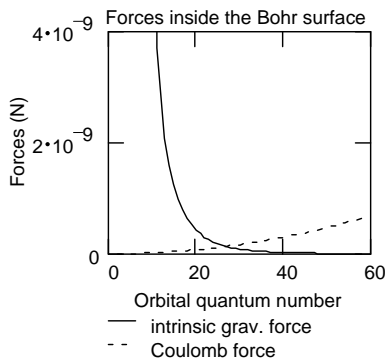


Fig. 7.16
Plots of IG and Coulomb forces
(drawn as continuous plots)

It become evident, that the slight increase of the electron velocity for $n > 26$, as shown in Fig. 7.15, is contributed by the increased Coulomb forces, as shown in Fig. 7.16.

Fig. 7.17 shows plots of the Coulomb forces for two cases: 1 - $F_c(2) = 0$; 2 - $F_c(2) > 0$ ($n = 2$ corresponds to the Balmer GS orbit).

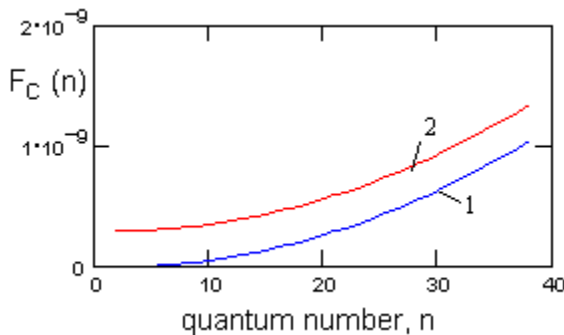


Fig. 7.17. Coulomb forces in function of quantum number (drawn as continuous plots)

Having in mind that the GS orbit is determined by the finite distance r_o , (see Fig. 7.11), it becomes apparent, why Coulomb force for $n = 2$ may not start from zero, but from some finite value. For this reason, the plot 2 is more probable. It does not affect significantly the curve shape of the energy level fitting, but may affect slightly the total orbital time, discussed in §7.8.3

The inertial mass dependence on the quantum number influences the shape of the velocity and energy levels of the series. The best fitting result is obtained for a second order inertial mass dependence, given by Eq. (7.11). Expressed in function of quantum numbers, the plot of Eq. (7.11) is a mirror image of the Coulomb forces expressed by Eq.(7.10). The plot of the inertial mass expression (7.11) is shown in Fig. 7.18.

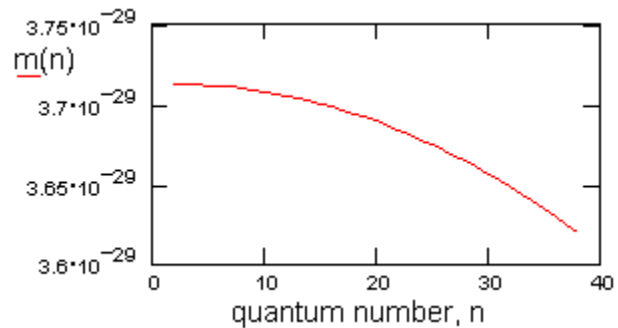


Fig. 7.18
Newtonian inertial mass of the electron
in the E-field quasishrunk space inside
the Bohr surface (drawn as continuous plot)

Using the obtained expressions of the inertial mass and velocity as functions of the quantum number, we may express the electron kinetic energy in eV, for any one of the quantum orbits by using the well known classical equation:

$$E_k(n) = 0.5m(n)v^2(n)\frac{1}{q} \quad (7.20)$$

The energy levels, according to the quantum mechanics are the potential energies, but referenced to the limit orbit. So we have:

$$E_p(n) = 0 - E_k(n) = -(0.5m(n))v^2(n)\frac{1}{q} \quad (7.21)$$

Fig. 7.19 shows the plot of the calculated energy levels, $E_p(n)$, together with the plot of the energy levels, $E_b(n)$, estimated by the spectral data.

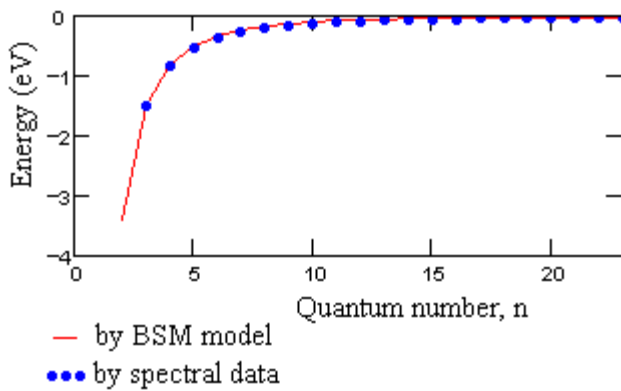


Fig. 7.19

Calculated and experimental energy levels for Balmer series

The shape of the calculated energies fits quite well to the levels from the experimental data (quantum mechanical levels). We also see, that we have referenced the model velocity only for $n = 2$, but the obtained energy range spans well for all Balmer series. The small discrepancy between the calculated and the experimental data might be contributed by:

- using idealised shape of the quantum orbit, as shown in Fig. (7.9)

- The IG law through LC space is different than in the empty space. In the former case the leaked IG forces dependence in close distance is inverse proportional to a distance at power larger than 3. The power index is also dependable on the absolute distance value.

The Balmer model output parameters for the best fit, shown in Fig. 7.19 are following:

$k_{qs} = 7.728$ - a quasishrink ratio, valid for the peripheral magnetic lines from the spin momentum (referenced to Bohr surface)

Quantum orbits: 37 ($2 < n < 38$)

$P = 5.474$ - degree of inverse power IG low through CL space

7.8.2.A Discussions:

The quantum efficiency for pumping the CL space is not considered in the Balmer model. When investigating the molecular vibrational spectra in Chapter 9, we will see, that it affects the CL space pumping. Then in the Balmer model, the quantum

efficiency will be a hidden parameter. This might be the reason, why a velocity minimum appears at $n = 24$. It could be explained by the shape of the orbit. At $n = 24$ the orbital shape approaches the Hippoped curve with parameter $a = \sqrt{3}$ and the distance between the locuses of the Hippoped curve - closer to the distance d (see Fig. 7.13). The quantum efficiency at such shape of the orbit might be a maximum.

The BSM model provides energy levels, consistent to the levels, obtained by the optical spectrum (Fig. 7.19). So the velocity concept may be considered as a correct parameter, including the quantum efficiency as a hidden one. Then we may calculate the quantum magnetic radius, by Eq. (3.39) from Chapter 3. For velocity value of $1.079E4$ m/sec corresponding to $n = 24$ we obtain for the small magnetic radius:

$$(r_{eq} = 5.194 \times 10^{-13}) \text{ m.}$$

Then the external magnetic radius is:

$$(R_c + r_{eq}) < 1.2 \times 10^{-12} \text{ m}$$

The quantum magnetic radius of the quantum orbits with lower quantum number is even smaller. **Consequently the quantum magnetic radii for all orbits of the series are inside the Bohr surface.**

Note: The quantum magnetic radius is estimated by the analysis in Chapter 3, where a repeatable motion in a quantum loop is not taken into account.

The Balmer model unveils one specific feature of the orbiting electron. When the electron drops to lower orbit, despite the fact that it obtains a larger velocity, its potential energy is lower, due to the IG forces. When such transition occurs, the energy difference will be emitted to the external space as a quantum EM wave - a photon. **Consequently the emitted photon carries a portion of potential energy, belonging to the IG forces between the electron and the proton.**

The above conclusion is of great importance, because it is valid for the energy levels of all atoms. **In fact the weight of the IG energy contribution increases with the Z number of the atomic element.**

The electron's geometrical parameters, valid for free CL space has been used without change in the model. Consequently, the fine structure constant, which appears as embedded parameter of the

electron geometry is also not changed inside the Bohr surface. The both proper frequencies of the electron as a system are also unchanged. These results obtained for the volume of the spectral line orbits should be also valid for the total volume inside the Bohr surface.

Investigating the separate contributions for the shape of the Balmer plot we may see that the change of inertial mass could not affect significantly the output result. The main contributors are the IG field and E-field. The E-field in fact is controlled by the IG field due to the charge unity mechanism. Consequently:

- **the energy of the orbiting electron is defined mainly by the IG energy of the system.**

This feature may be considered valid also for the heavier atoms where the IG energy of the nucleus contributes to the energy of detected emitted or absorbed photon. (In such aspect the inertial mass contributes only a small correction on the cenrapetal acceleration force).

The above conclusion is one of the major distinct parameter between the BSM model and the Bohr model of the Hydrogen atom. This leads to the following major distinctions between both models:

Summary:

- **Major distinctions between Bohr model of Hydrogen and BSM model:**
 - In the Bohr model, the orbit with a length of $2\pi a_o$ is the most internal orbit.**
 - In the BSM model, the orbit with a length of $2\pi a_o$ is the most external possible orbit**
- **The spectral line positions in the series carry signatures of: the IG field, the E-field, and the electron inertial mass inside the Bohr surface**
- **The resolvable spectral lines are in the range of velocity inversion**
- **The magnetic radius of the electron for all quantum orbits could not appear outside of the Bohr surface.**
- **The two proper frequencies of the electron as a system are not affected by the properties of the space volume enclosed by the Bohr surface.**

7.8.3 Orbital time

From the concept of CL space pumping and Balmer series model it is apparent that the CL space is pumped during orbital circling of the electron, and after the electron falls to a lower orbit the pumped energy is emitted as a photon (quantum wave). The well determined energy of the photon indicates that the electron makes a whole number of orbital cycles. This is in agreement with the relation between conditions of whole number of cycles discussed in §7.7.1. This relation is shown in the following table:

Phase repetition condition	e- rotations	internal positron-core cycles
short time	18778.3(3)	56335
long time	56335	2573380

The phase repetition time could be considered as a necessary but not enough condition for the finite time of the electron on orbit. In the Quantum mechanics (QM) this time is known as a lifetime in activated state. It is a constant for a spontaneous emission, while it is shorter for stimulated emission used in lasers. The QM could not provide an explanation of the physical mechanism, that determine this time. Now the possible explanation could be given for a first time.

The condition that defines the limit time duration of the orbit according to BSM is reduced to a possible number of full orbital cycles according to the considerations of the phase repetition. The second factor that may influence the possible number of orbits could be related to the short magnetic line condition. This condition is valid simultaneously for the axial and peripheral magnetic lines created from the electron's motion. While the axial lines are related with the λ_{SPM} , valid for the external free CL space, the peripheral lines are related with the shrunk λ_{SPM}' valid for the orbital space inside the Bohr surface. Obviously both conditions comes in conflict after some finite time from the beginning (when the electron start circling in the particular orbit). This could be inferred from the analysis of the relation between the CL space relaxation constant and orbital time for the two cases: axial and peripheral magnetic lines.

For the axial magnetic lines the CL space constant is t_{cl} . For the peripheral magnetic lines the quasishrunk CL space constant follows the same dependence on the distance from the proton core as the parameter λ_{SPM} given by Eq. (7.15).

The orbital time from the Balmer model is obtained by division of the orbital length (Eq. 7.16) by the orbital velocity (plotted in Fig. 7.1).

$$t_{orb}(n) = \frac{L_{orb}(n)}{V(n)} \quad (7.23)$$

Two plots of Eq. (7.23) for short magnetic line conditions: applied for axial and peripheral magnetic lines are shown in Fig. 7.20. The time scale is multiplied by factor of 3 for a reason explained later.

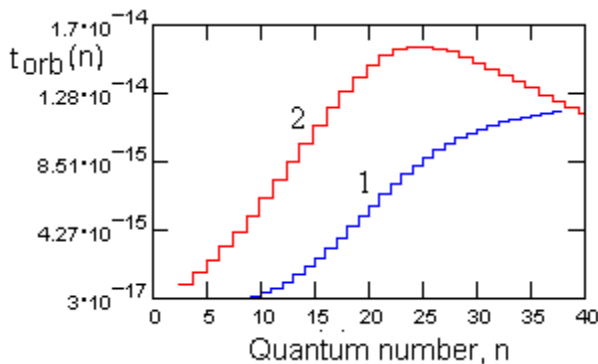


Fig. 7.20

Trend of the short magnetic line conditions in function of quantum number
 1- for the peripheral magnetic lines
 2- for axial magnetic lines
 The quantum numbers are in the scale of curve 2, related to the quantum number of the orbit.

We see from the plot that the trends of the two curves are different. While their relative position might be influenced by the properly determined quasishring index, their trends will be always different. But this difference means that a conflict between the two types of magnetic line conditions may occur for a finite time of the electron on the particular orbit. The quantum features of the CL space and the electron system oscillation may make the conflict to occur in the time when the oscillation passes through the initial phase. Then the electron falls to lower orbit. The most probable lower orbit is the ground state orbit of the series.

The provided considerations has to been combined with the conditions of the phase repetition between the two proper frequencies of the electron and the CL node Compton frequency. This issue has been discussed in §3.12.2.A.

The developed concept is valid for a single Hydrogen atom only. The obtained lifetime should not be confused with the cases of long lifetimes for some atoms or molecules. In the latter cases quite long lifetimes may result from different mechanisms involving complex interactions between multiple orbits.

Summary:

- **The spontaneous life time is defined by the mechanism of the short magnetic lines, strobed with the effect of the phase match conditions between the two electron proper frequencies and the Compton wavelength of the CL nodes**
- **In case of spontaneous emission the lifetime of the exited state for Balmer series is equal to three orbital cycles of the electron.**
- **The orbital time could not be shorter than one orbital cycle of the electron**
- **The finite lifetime is a result of conflict between axial and peripheral short magnetic line conditions, developed for a finite time of the electron motion in the proton E-field.**

7.9. Photon emission and absorption. Physical explanation of the uncertainty principle.

Let analyse the electron motion in one orbit of Balmer series above the GS orbit. The induced peripheral magnetic lines by the spinning electron are in the region inside the Bohr surface. During the stable motion of the electron, the Hydrogen appears neutral outside the Bohr surface. Consequently the electron momentum is able to neutralize the distributed E-field lines inside the Bohr surface. The CL space interaction will balance this momentum, so it will contain a balance energy. This energy is distributed in the orbital trace, formed by the electron quantum magnetic radius (see Fig. 7.7). **The energy, kept in the volume swapped by the magnetic radius is possible due to the shorter refreshing cycle, supported by the orbiting electron.** Due to the finite orbital time, determined by the short magnetic line condi-

tion conflict (described in the previous paragraph), the motion in a given orbit may be terminate by two possible ways:

(a) the electron falls to lower orbit

(b) the electron jumps to higher orbit, if the proton club space has received external energy in a proper time.

Photon emission. The case (a) mentioned above is related with a photon emission. The termination of electron motion in the current orbit terminates the volume energy refreshing. The excess energy is a difference between the electron energies in the two orbits. This energy distributed in the former trace is in conflict with the proton E-field inside the Bohr surface. Now regarding the excess energy volume as running EQ's they are pushed in direction to less intensive IG field (for the line series, the IG field predominates the E-field). The running EQ's carrying an excess energy above the ZPE, are refurbished in a quantum wave (photon), with wavelength corresponding to the total excess energy. The most probable transition to lower orbit is the transition to the GS orbit of the series. In this case the conditions of quantum orbit are always present. This is the case of spontaneous emission. For any other transition to orbit higher than the GS additional conditions are needed.

Photon absorption. An electron in a lower orbit may jump to a higher one, if obtaining an energy in a proper time, referenced to its orbital time. This is a process of absorption. The absorption of photon, also is not instantaneous process. It may involve number of orbital cycles. It is well known from the quantum mechanics and the experiments, that the total energy of the photon is transmitted to one electron. But how the energy of the quantum wave wavetrain occupying much larger volume than the proton, is shrunk into the internal space of Bohr surface? The only possible option is to accept an **energy dumping effect** of the combination of the proton space inside the Bohr surface and the orbiting electron (in analogy with a dumping effect for mechanical waves, propagated in a stiff media). If considering a solid optical detector, the size of the quantum wave usually covers many protons with their Bohr surfaces. In order to start the dumping effect, however, the orbiting electron has to posses a proper phase referenced to the proton club and matching the quantum time condition. Then

the energy dumping effect selectively starts for one electron, whose quantum orbit conditions are closer. Once the dumping is started, the whole energy of the quantum wave is sucked, contributing only to the energy of this electron. The process is not simple and may involve number of nonlinear factors inside the Bohr surface. The intuition for a possible nonlinear factors comes close to mind if analysing the experiment described by L. J. Wang et al. (2000).

Heisenberg uncertainty principle. The emission and absorption processes are able to provide explanation of the Hisenberg uncertainty principle, applied to the electron motion in the atoms. It is evident, that emission and absorption processes are related with many orbital cycles. The both processes have a finite time duration. **The receiving system, however, will get the energy only at the end of the process.** In a case of a real detection system, **even with a super fast detector, the detector system will get the energy only when the electron quits the orbit (the corresponding atom is ionized).**

CL space pumping. If the electron in GS orbit, for example, gets some energy from absorbed photon, it jumps to a proper higher orbit, but stays here a finite time and returns back, most probably to the GS. In this case the same obtained energy is reemitted. We may regard the process as a CL space pumping, a terminology, used in previous chapters. Variety of CL space pumping processes exist, some of which, have been already discussed. One of them was the CL space pumping in the positronium (see §3.17.3). There is one common feature between both processes of CL space pumping. In the positronium transition $1^3S_1 - 2^3S_1$, the emitted photon energy is $(13.6 - 3.4)/2 = 5.1$ eV. So it is referenced to the common centre of mass in respect to the fixed CL nodes of the laboratory frame.

In the case of Hydrogen atom, the proton mass is much larger than the electron one, and the proton could be considered as a carrier of local frame. In case of the Ps $1^3S_1 - 2^3S_1$ transition (see §3.17.3), both, the electron and the positron are oscillating. Their centre of mass, however, is determined by their different quantum velocities, corresponding to 13.6 eV and 3.4 eV. They have one and a same inertial mass but oscillating around a common centre of mass with different velocities.

In fact the common centre of mass is not fixed in CL space, but oscillating. For this reason the difference between 13.6 and 3.4 eV is additionally divided by two. The physical explanation of this effect without taking into account the CL space is not possible.

Some very low energy photons, from the Hydrogen emission spectra, also may get physical explanation, when considering the CL space interaction. During the photon emission the Hydrogen atom gets a kick in opposite direction. Due to the orbital quasiplane twisting shape, the Hydrogen gets simultaneous spin momentum. This momentum may cause emission of another quantum wave, with much lower energy. This may explain the Hydrogen emission at 21 cm coming from the space.

7.10 Electron spin and fine structure line splitting

According to the quantum mechanics, the electron motion is characterized with two spin values. Let call this parameter a QM spin, in order to distinguish it of from the spin momentum, that is an angular momentum of the electron confined motion. But what is the physical meaning of QM spin?

The QM spin is initially introduced with purpose to explain the spectral line splitting of the line series. This splitting is larger for transitions between orbits with lower quantum numbers. This feature indicates that the QM spin is related to the velocity direction, referenced to the proton club quasiplane. The quasiplane has a twisted shape, determined by the twisted shape of the proton core. It is enough correct to say, that the quasiplane posses a chirality determined by the twisted shape of the proton. This chirality, namely, is a reference point, allowing two opposite QM spins value to be distinguished. For orbit with one and a same quantum number the orbiting electron may move in two different directions, distinguished by the proton handedness. Its energy in both cases, however, should be slightly different. Such energy difference is detected by as closely separated spectral lines. The separation is larger for orbits closer to the proton core, because IG field is stronger in this region. This effect is known as a **fine structure line splitting**.

All this considerations are valid only in electron motion in quantum loop, and when the shape of the loop is defined by a presence of a proton. For motion in open trajectory away of the definition conditions of the proton, the QM spin losses a sense. It should not be confused with the electron system polarization effect, characterized with invoked radial motion of the internal positron, after an electron beam is reflected by a solid surface under angle.

Summary:

- **The QM spin is a physical parameter related to the match or mismatch between the chirality of the electron spin rotation and the chirality of the proton.**

7.11 Pauli exclusion principle. Magnetic fields inside the Bohr surface.

According to Pauli exclusion principle one orbit could be occupy by no more than two electrons. When the orbit is occupied by two electrons, they have opposite spin.

These conditions are reasonable, for all kind of orbits, passing through the proton club. In BSM concept the opposite spins means, that the two electrons circle the same orbit but in opposite directions. In Balmer orbits they pass simultaneously through the proton clubs near the locus. However they do not collide because:

- the guiding role of the magnetic field and the repulsion of the E-field of the electrons
- the orbits are pretty close, but not exactly the same due to the interaction between the axial spin of the electron and the helicity of the proton.

The motion of two electrons in a common orbit is illustrated by Fig. 7.21.

The instant positions of the two electrons become synchronized each other, so in any moment they have symmetrical positions, referenced to the quasiplane of the proton club. The instant symmetry in one particular moment is illustrated in Fig. 7.21. We see that a kind of symmetry exists between two electrons in one orbit. This symmetry in fact is supported by the induced magnetic field.

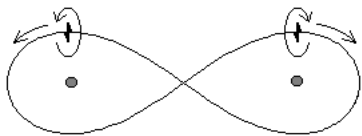


Fig. 7.21

Instant position symmetry of two electrons with opposite QM spin, occupying one quantum orbit of Balmer series

It is evident, why the two electrons can't possess one and a same spin. The opposite QM spins allow their magnetic fields from the orbital motion to be mutual compensated with a symmetry referenced to the proton club. The magnetic lines of these fields are normal to the orbital plane. We may call this field an **orbital magnetic field**. This field has a different configuration than the magnetic field induced by the spin (rotation) momentum of the electron. In the vicinity of the electron, the magnetic lines of the both fields are normal each other and do not interfere. The orbital magnetic field, however is created in a E-field CL space, inside the Bohr surface, where the $\lambda_{SPM'}$ is different than the λ_{SPM} of the external CL space. **For this reason the created magnetic lines may not be able to make paths outside of the Bohr surface.** Therefore, they are closed inside. This feature explains the fact that the orbiting electron does not exhibit external magnetic field. This is valid not only for single, but also for pair electrons that convert the atom to a negative ion. The negative ion possesses completely symmetrical charge feature as the positive one, despite the completely different dynamics inside the Bohr surface.

From the above analysis it becomes evident that similar conditions for more than two electrons are not possible. Said in a simple way, two electrons "complete" the orbit (according to the Pauli exclusion principle), because no more than two orbits of opposite Quantum Mechanical spin are possible.

Summary:

- **Physical meaning of the Pauli exclusion principle: two electrons with opposite QM spins posses two individual symmetrical orbits with one and a same orbital quantum condi-**

tions. Such conditions are not possible for more than two electrons, because the magnetic field symmetry is disturbed.

- **The orbital magnetic field from one or pair electrons in the orbit is enclosed inside of the Bohr surface, due to the different SPM frequency of the E-field CL space from the external free CL space.**
- **The negative ions does not exhibit external magnetic field despite the second orbiting electron, for the same reason.**

7.12 Superfine spectral line structure

During the photon emission, the excess energy kept so far inside the Bohr surface gets a fast escape as an emitted photon. The local gravitational field of the proton serves as a reference frame. It is reasonable to consider, that the proton exhibit reaction force during the moment of the photon shot. Due to its large inertial mass it gets a slight kick. Its helicity and twisted orbital shape of the circling electron, converts part of the kick momentum to a nuclear rotation. The emitted quantum wave have a finite wavetrain length and consequently a finite emission time. So the kick effect is able to influence the photon emission, providing in such way a small frequency shift, as a red Doppler shift. In the same time the proton has some left over energy as a small spin momentum. In some moment this rotational momentum may become in conflict with the orbiting electron. The atom could free this energy only as an emission of a low energy quantum wave. The energy of the emitted in this case photon, however, depends also on the current status of the QM spin of the electron. The signature of this dependence is **the superfine spectral line structure.**

In the atoms with higher Z number, the superfine structure may have more splittings, due to the orbital interactions effect. The latter is discussed in Chapter 8.

7.13 Lamb shift

In QED the Lamb shift is known as displacement of the GS (ground state) level from its position, estimated by the difference between the expected energy level and the real one. This is observable from Hydrogen to higher Z number of el-

ements. The Lamb shift increases with the Z number.

Let considering the Balmer series. The orbital shape and dimensions of all orbits in the series with exception of the GS orbit are defined only by the quantum conditions. Only for the GS orbit additional conditions appear for termination of the quantum loop condition. It is related with the quantum magnetic radius interference with the proton core (see §7.8 and Fig. 7.11). So it is very reasonable the lowest orbit quantum condition (corresponding to the GS) to appear slightly displaced. The orbit deformation gives slight shift of the quantum position, estimated by the Quantum mechanical model. The deviation from the exact quantum value becomes observable, because this orbit is closer to the proton core. In this range the IG forces are stronger and are proportional of higher inverse power degree of the distance. For a similar reasons, the orbit deformation and the quantum shift for GS orbits in atoms with higher Z numbers is larger. It is also evident, that the Lamb shift may appear only for GS orbits near the proton core. This condition is valid not only the Lyman and Balmer GS orbits in the Hydrogen, but also for the corresponding similar orbits in the heavier elements.

7.14 Zeeman and Stark effects.

The Stark effect is a spectral line splitting as a result of applied electrical field. The Zeeman effect is a spectral line splitting as a result of applied magnetic field. In fact the Zeeman effect could be also a line shifting. The detection effect may provide a signature of line splitting as a result of the following conditions:

- detection of photons from different atoms
- consecutive photon detection from one and same atom but with different orientations in respect to the applied field

In order to explain the physical process, we will use the term line shifting. There are two major differences between the both effects. In the Zeeman effect, two different type of shifting are observed: for small and for large intensity magnetic field. The Stark effect does not exhibit such phenomena. These differences helps to identify the physical process.

In the Stark effect, the applied electrical field deforms the shape of the Bohr surface. This may influence the position of the quantum orbits. The orbital energy level is very dependent of its position, because the strong gradient of the IG field. The gradient is also larger for orbits with low quantum numbers.

In the Zeeman effect, the applied magnetic field could not influence the Bohr surface. The Bohr surface, by definition, is generated by the static E-field of the proton and should be not affected by a magnetic field. **The applied magnetic field, however, may generate magnetic lines inside the surface, that could influence the orbital quantum conditions.** The penetrating magnetic lines may obtain loops closely to the magnetic fields generated by the orbiting electron. Having in mind the both quantum conditions, defining the quantum orbit (see § 7.7.3), it is close to the mind, that the two types of the Zeeman effect are related with them:

- (a) caused by low intensity magnetic field
- (b) Caused by high intensity magnetic field

The low intensity magnetic field may not influence the short magnetic line quantum condition, related with the axial magnetic lines of the electron. The volume of this field possesses very small thickness (smaller than the Compton radius). But it may affect the quantum loop condition, of peripheral magnetic lines, whose volume is much larger.

The higher intensity magnetic field may affect the both type of short magnetic line quantum conditions. Having in mind, that the SPM frequencies of the applied magnetic field and the axial magnetic lines are both equal, the stronger field may provide a different type of line shifts in comparison the weaker one.

7.15 Cross validation of the Hippoped curve concept, for the shape and dimensions of the proton and the quantum orbits.

Here we will summarize, briefly, the cross calculations and validations, some of which are used so far and others - given in the next Chapters. The knowledge of the shape and dimensions of the proton, neutron, electron, and the quantum orbits, is very useful for understanding the structure of the

atomic nuclei and their physical and chemical properties.

A. Shape and dimensions of the electron as a system of three helical structures with internal rectangular lattice (twisted)

- Static and Dynamic CL pressure expressed by the electron volume and surface, involving the Compton radius (wavelength) Plank constant, light velocity and fine structure constant
- Magnetic radius, calculated by the magnetic moment the Compton radius and number of physical constants
- Relation between the electron static charge and the quasiparticle waves in the beta decay (virtual electron and positron)
- X-ray properties of the electron
- Electron system modifications and proper frequencies validation by experimental data of FQHE
- CL space pumping and proper frequency validation by the Positronium
- Electron system modification in Superconductivity state of the matter
- Internal gravitational lattice structure validation by the destruction energy (tau lepton at 1.7778 GHz and the resonance at 1.44 GHz
- electron and muon magnetic moments, mass ratio and their physical meaning
- derivation of relativistic gamma factor by the dimensions and property of the moving and oscillation electron
- quantum motion of the electron and its confined motion in a quantum, as a property of the quantum orbit

B. The proton shape and dimensions

- Matching the proton dimensions to the calculation of the temperature of 2.72K with the experimentally measured one in which the ideal gas constant and Avogadro's number are involved, together with other physical constants (Chapter 5);
- matching the mass ratio of the pion to muon; the magnetic moment ratio between electron and muon; mass balance equation of the proton (involving all pions and kaon); mass balance equation of eta particle; stopping ratio between proton and antiproton; relation between Newtonian mass

change due to FOHS twisting and electroweak parameter $\theta_{eff}^{lept} = 28.762$ deg and Fermi coupling constant; internal FOHS destruction energy ratio between right and left handed structures, by tau lepton equivalent mass energy at 1.7778 GeV and the resonance energy at 1.44 GeV; the destruction energy of untwisted K+ and K- (kaons) matching to W+/- bosons; destruction energy of twisted K- by Z boson; prediction of the destructive energy of twisted K+ at 105 GeV; physical explanation of the relation between the muon lifetime, Fermi coupling constant and pion muon electron decay

- matching the proton dimension to the Balmer model

C. Neutron shape and dimensions

The dimensions of the neutron are obtained directly from the proton, because the external difference is only in their shapes. While the proton is a torus, but twisted in a shape of hippoped curve, the neutron is a folded torus with a shape of a double rings (with some small gap between the two loops).

D. Proton and quantum orbit dimensions

- matching the proton and quantum orbit dimensions for atoms in molecules (Chapter 9)
- matching the dimensions calculated for H₂ molecule ortho state and cross validating them by data from optical molecular spectra and photoelectron spectroscopy (Chapter 9).

Notice

In all cross validations only accurate physical constants and reliable experimental data are used. All the sources of experimental data are referenced. The inclusion of CL space concept, helps to explain the relation between the electric, magnetic and gravitational fields. It allows to explain also the fundamental quantum mechanics rules, and the relativistic features in a classical way. The dimensions and structure of the atomic and subatomic particle appears quite different, than the existing so far models and theories. The BSM models, however matches quite well with the experimental data and the observations from different physical fields.